

IGR J19308+0530: Roche lobe overflow on to a compact object from a donor 1.8 times as massive[★]

E. M. Ratti,^{1†} T. F. J. van Grunsven,^{1,2} M. A. P. Torres,^{1,3} P. G. Jonker,^{1,2,3}
J. C. A. Miller-Jones,⁴ J. W. T. Hessels,^{5,6} H. Van Winckel,⁷ M. van der Sluys^{2,8}
and G. Nelemans^{2,7}

¹*SRON, Netherlands Institute for Space Research, Sorbonnelaan 2, NL-3584 CA Utrecht, the Netherlands*

²*Department of Astrophysics/IMAPP, Radboud University Nijmegen, Heyendaalseweg 135, NL-6525 AJ, Nijmegen, the Netherlands*

³*Harvard-Smithsonian Center for Astrophysics, 60 Garden Street, Cambridge, MA 02138, USA*

⁴*International Centre for Radio Astronomy Research – Curtin University, GPO Box U1987 Perth, WA 6845, Australia*

⁵*ASTRON, the Netherlands Institute for Radio Astronomy, Postbus 2, NL-7990 AA Dwingeloo, the Netherlands*

⁶*Astronomical Institute ‘Anton Pannekoek’, University of Amsterdam, Science Park 904, NL-1098 XH Amsterdam, the Netherlands*

⁷*Instituut voor Sterrenkunde, KU Leuven, Celestijnenlaan 200D, B-3001 Leuven, Belgium*

⁸*Nikhef National Institute for Subatomic Physics, Science Park 105, NL-1098 XG Amsterdam, the Netherlands*

Accepted 2012 December 23. Received 2012 December 19; in original form 2012 November 6

ABSTRACT

We present phase-resolved spectroscopy and photometry of the optical counterpart to the X-ray binary IGR J19308+0530. Ellipsoidal modulations in the light curve show that the F-type companion star in the system is Roche lobe filling. The optical spectra are dominated by absorption features from the donor star, with ~ 10 – 20 per cent disc contribution to the optical continuum. We measure an orbital period of 14.662 ± 0.001 h, a radial velocity semi-amplitude for the companion star of $K_2 = 91.4 \pm 1.4$ km s^{−1} and a rotational broadening of $v \sin i = 108.9 \pm 0.6$ km s^{−1}. From K_2 and $v \sin i$, given that the donor star is filling its Roche lobe, we derive a mass ratio of $q = M_2/M_1 = 1.78 \pm 0.04$, which is typically considered to be too large for stable Roche lobe overflow. Our observations support an inclination of $\sim 50^\circ$. The accretor in IGR J19308+0530 is most likely a white dwarf, although a neutron star cannot entirely be excluded.

Key words: accretion: accretion discs – stars: individual: IGR J19308+0530 – X-rays: binaries – novae, cataclysmic variables – stars: mass loss.

1 INTRODUCTION

Intermediate-mass X-ray binaries (IMXBs) are binary systems where a compact object – black hole (BH), neutron star (NS) or white dwarf (WD) – is accreting matter from a companion star of spectral type A or F. IMXBs are rarely observed [see, e.g. the catalogue from Liu, van Paradijs & van den Heuvel (2007) and the 2012 version of the RK catalogue Ritter & Kolb (2003)].¹ The majority of accreting WDs in binaries, in fact, belong to the class of cataclysmic

variables (CVs), which have late-type secondaries ($M_2 \lesssim M_1$) and $P \lesssim 6$ h (Knigge, Baraffe & Patterson 2011). NSs or BHs, instead, are typically observed in X-ray binaries (XRBs) hosting either a massive O-B donor star (high-mass XRBs, HMXBs) driving accretion via stellar wind, or a late M or K dwarf secondary star (low-mass XRBs, LMXBs) accreting via Roche lobe overflow. The reason for the observed rarity of IMXBs especially among NS and WD systems is that, when the companion is more massive than the accretor but not massive enough to have strong winds, wind accretion proceeds at a very low rate and Roche lobe accretion is thought to be unstable. For NSs and WDs in IMXBs mass flows from the more massive to the lighter star and angular momentum conservation shrinks the orbit, leading to enhanced mass transfer. The bright XRB phase is therefore intense and short lived, causing an observational bias towards LMXBs, CVs and HMXBs (Tauris & van den Heuvel 2006). Nevertheless, IMXBs could be a large fraction of the XRB population and have an important role in understanding their evolution (Podsiadlowski, Rappaport & Pfahl 2001). Cyg X–2 and Her X–1 are thought to have started as IMXBs, even though the measured mass ratio is currently < 1 .

[★]Observations made with the HERMES at the Mercator Telescope, operated on La Palma by the Flemish Community, at the Spanish Observatorio del Roque de los Muchachos of the Instituto de Astrofísica de Canarias. HERMES is supported by the Fund for Scientific Research of Flanders, the Research Council of KU Leuven and the Fonds National Recherches Scientifique (FNRS), Belgium, the Royal Observatory of Belgium, the Observatoire de Genève, Switzerland and the Thüringer Landessternwarte Tautenburg, Germany.

[†]E-mail: e.m.ratti@sron.nl

¹<http://physics.open.ac.uk/RKcat/>

IGR J19308+0530 was discovered by *INTEGRAL* (Bird et al. 2006) and observed by *Swift* (Rodríguez, Tomsick & Chaty 2008). An association with the star TYC 486-295-1, classified as an F8 star in the survey by McCuskey (1949), was made using the *Swift* position (Rodríguez et al. 2008). This was confirmed using an accurate *Chandra* position of the X-ray source (Ratti et al. 2010). Considering typical parameters of an F8 star, Rodríguez et al. (2008) suggested IGR J19308+0530 to be an L/IMXB in quiescence or a CV at a distance of $\lesssim 1$ kpc.

Here, we present phase-resolved optical spectroscopy and photometry of IGR J19308+0530, in order to measure the orbital period P , the radial velocity semi-amplitude K_2 and the projected rotational velocity $v \sin i$ of the companion star, and the system inclination i . In a Roche lobe filling system, K_2 and $v \sin i$ allow us to infer the ratio $q = M_2/M_1$ between the mass of the secondary and the primary star in the system (Wade & Horne 1988, see also Gray 1992) and, knowing P and i , to solve the system mass function.

2 OBSERVATIONS AND DATA REDUCTION

In total 22 high-resolution spectra of IGR J19308+0530 were collected. Observations were made on two nights in 2010 March, one night in 2010 April and 9 nights in 2010 June using the fibre spectrograph High Efficiency and Resolution Mercator Echelle Spectrograph (HERMES), mounted at the Mercator telescope in La Palma (Raskin et al. 2011). The typical exposure time was 1200 s. The spectra have a dispersion of 0.027 \AA/pixel at 5000 \AA and cover the wavelength range $3770\text{--}7230 \text{ \AA}$. The fibre aperture is 2.5 arcsec on the sky, but the presence of a slicer mimics a narrow slit providing a resolution of $\sim 85\,000$ irrespective of the seeing. The template star HD 185395, of spectral type F4 V (later found to be the closest match to the spectral type of the target, see below) was observed with the same settings for 360 s on 2009 August 5. The extraction of the spectra was performed through the dedicated automated data reduction pipeline HermesDRS. For each spectrum we selected two regions for the analysis, one covering the $H\gamma$ and $H\beta$ lines ($4280\text{--}5250 \text{ \AA}$) and one around the $H\alpha$ line ($5950\text{--}6700 \text{ \AA}$), which we will refer to as S1 and S2, respectively. These regions were selected as they are rich in stellar lines, with little contamination from interstellar features. A good fit of the continuum was achieved in each region with a polynomial function of order 9. We normalized the spectra dividing by the polynomial fit.

We also performed time-resolved photometry of IGR J19308+0530, with the 80 cm IAC80 telescope at the Observatorio del Teide in Tenerife equipped with the CAMELOT CCD imager. The observations were obtained during part of three nights between 2010 July 30 and August 02, by cycling through the Sloan g' -, r' -, i' - and z' -band filters. Three consecutive exposures were obtained in each filter, with integration times ranging from 6 to 24 s depending on the filter and seeing conditions. Standard stars were not taken due to non-photometric weather. After debiasing and flat fielding the images using dome flat-field observations (with standard routines in IRAF), the instrumental magnitudes of IGR J19308+0530 and four comparison stars were computed by means of aperture photometry. Differential light curves were then obtained for IGR J19308+0530 with respect to the comparison star TYC 486-968-1. We also extracted light curves for TYC 486-968-1 using the other comparison stars. No significant variability was detected in the i' band ($\text{rms} \lesssim 0.006 \text{ mag}$), whereas for the other bands a larger scatter was observed due to weather conditions (clouds and Calima). The maximum departure from the mean value was of 0.1 mag . Given

that the ellipsoidal modulation in IGR J19308+0530 is small in amplitude we decided to model only the i' -band light curves.

3 ANALYSIS AND RESULTS

3.1 Spectroscopy

The spectra are dominated by absorption features from the secondary star (Fig. 1). Although no emission line is directly visible, residual emission in the Balmer lines appears when subtracting one spectra from another, after correcting for the orbital shift of the lines. The emission component is variable in intensity and wavelength and slightly shifted with respect to the absorption line.

Using the package MOLLY developed by T. Marsh, we measured the orbital velocity of the companion star in IGR J19308+0530 by cross-correlating the spectra of the target with that of the template star. As the absorption lines are rotationally broadened in the target spectrum, a broadening of 100 km s^{-1} was applied to the template (see below on rotational broadening), improving the cross-correlation. The Balmer lines and interstellar features were masked.

We performed a fit of the velocities versus time with a sine function, with K_2 , the systemic radial velocity γ , T_0 and P as free parameters. T_0 was constrained to be near the middle of the time span over which the observations were taken, and such that phase 0 is at the inferior conjunction of the companion star. The best-fitting sinusoid provided a χ^2 of 57.6 for the region S1 and 41.76 for S2 (19 d.o.f.). In both cases, the uncertainties on the parameters were estimated assuming that the sinusoidal model was correct, and we scaled the errors on the velocities to reach a reduced χ^2 of ~ 1 . The values of P , T_0 and γ measured in S1 and S2 are consistent at the 1σ level, K_2 is consistent at the 2σ level. The error-weighted average of the parameters gives $P = 0.61092 \pm 0.00003 \text{ d}$, $T_0 = 2455330.8169 \pm 0.0023 \text{ HJD/UTC}$, $K_2 = 91.4 \pm 1.4 \text{ km s}^{-1}$ and $\gamma = -18.5 \pm 0.9 \text{ km s}^{-1}$. Fig. 2 shows the radial velocity curve (rv) folded on the above period. The value of γ is in the reference frame of the template star used for the cross-correlation, whose systemic radial velocity is $-28 \pm 0.9 \text{ km s}^{-1}$ (Wilson 1953). The

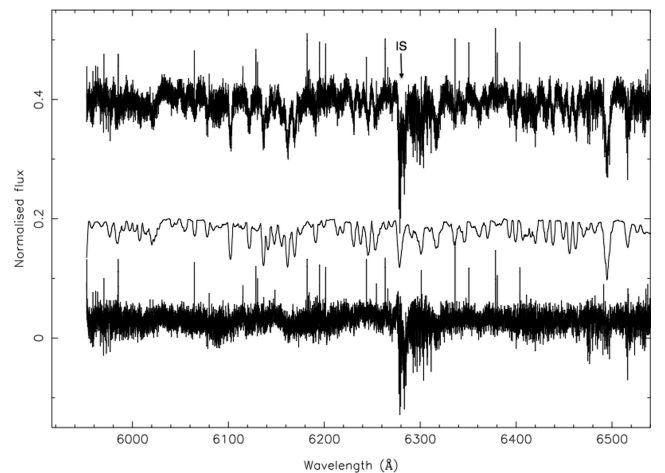


Figure 1. Optimal subtraction of the spectrum of the F4V stellar template HD 185395 from the spectrum of IGR J19308+0530. The image shows the part of spectral region S2 used to measure $v \sin i$. The interstellar feature at $\sim 6280 \text{ \AA}$ was masked. The template and target spectrum are offset by 0.4 and 0.2 in y.

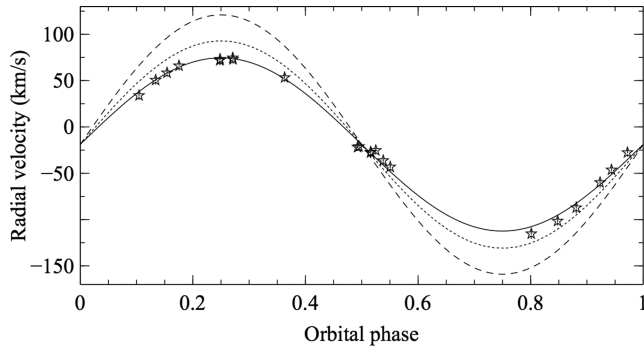


Figure 2. Radial velocity curve from the absorption lines in the IGR J19308+0530 spectra (region S1) and its best-fitting sinusoid (solid line). For comparison we plot circular orbits with $K_2 = 112 \text{ km s}^{-1}$ (dotted line) and $K_2 = 140 \text{ km s}^{-1}$ (dashed line), providing $q = 1.4$ and $q = 1$, respectively, for the observed $v \sin i$.

systemic radial velocity of IGR J19308+0530 is therefore $-46.5 \pm 1.2 \text{ km s}^{-1}$.

We obtained a set of high signal-to-noise template spectra from the UVES (Ultraviolet and Visual Echelle Spectrograph) Paranal Observatory Project (UVESPOP; Bagnulo et al. 2003) of A, F and early G stars of luminosity class V, III and IV. We subtracted each template spectrum from the Doppler-corrected average of the IGR J19308+0530 spectra between orbital phase 0.9 and 0.1. The reason for choosing this range in phase is that the oblate shape of the Roche lobe filling companion star and the possible presence of irradiation from the compact object could cause asymmetries in the line profiles, which are minimized close to phase 0. We performed a χ^2 test on the residuals of the subtraction: the template resulting in the minimum χ^2 provides our best estimate for the source spectral type. In particular, we adopted the optimal subtraction procedure implemented in MOLLY, where the templates are multiplied by a factor $0 < f < 1$ before the subtraction, representing the fractional contribution of light from the secondary star (1 minus the disc veiling). The factor f is found by minimizing the difference between the residuals and a smoothed version of itself. Before doing the subtraction, the UVESPOP spectra were shifted to the rest frame of the average target spectrum, and degraded to match the sampling and line broadening of the latter.

The procedure favours an F4-F6 V companion star, with a disc veiling of 10–20 per cent. The same spectral type and veiling are obtained when considering an average of the target spectra around phase 0.5, suggesting little irradiation on the inner face of the companion star.

To measure $v \sin i$, we compared the spectrum of the template star with the Doppler-corrected average of the IGR J19308+0530 spectra between phase 0.9 and 0.1. The observed full width at half-maximum of the absorption lines in the target spectra is determined by the intrinsic line width (expected to be dominated by $v \sin i$), broadened by the instrumental resolution profile and smeared by the motion of the companion star during the integration time of one observation. In order to account for the smearing, we made as many copies of the template spectrum as the number of target spectra we used for the average and we artificially smeared each copy of the template by $2\pi T K \cos(2\pi\phi)/P$, where T is the duration of one exposure on IGR J19308+0530 and ϕ the phase of one of the IGR J19308+0530 spectra we averaged. After that, we averaged the smeared template and broadened the resulting spectrum with different values of $v \sin i$. For each $v \sin i$, we performed an optimal

subtraction of the broadened template from the averaged spectrum of IGR J19308+0530: again the broadening which gives the minimum χ^2 provides a measure of the actual $v \sin i$ (Fig. 1). A value of 0.5 was assumed for the limb darkening. We masked interstellar features and the lines from the Balmer series.

In order to estimate the uncertainty on $v \sin i$, we included this procedure in a Monte Carlo simulation, following Steeghs & Jonker (2007). We copied each target spectrum 500 times, using a bootstrap technique where the input spectrum is resampled by randomly selecting data points from it. The bootstrapping maintains the total number of data points in the spectrum. For each bootstrap copy, one value of $v \sin i$ is measured as described above. The distribution of $v \sin i$ obtained from the 500 copies is well described by a Gaussian, whose mean and rms provide the best-fitting $v \sin i$ and its 1σ error. As template and target spectra are acquired with the same instrument, the instrumental resolution profile is not affecting our measurement.

The weighted average of the results from S1 and S2, consistent at the 1σ level, is $v \sin i = 108.9 \pm 0.6 \text{ km s}^{-1}$. With $v \sin i$ and K_2 , we calculated the system mass ratio $q = M_2/M_1$ from the relation $\frac{v \sin i}{K_2} = (1 + q) \frac{0.49q^{2/3}}{0.6q^{2/3} + \ln(1+q^{1/3})}$ (Horne, Wade & Szkody 1986), obtaining $q = 1.78 \pm 0.04$.

3.2 Ellipsoidal modulation and system inclination

Fig. 3 shows the i' -band light curve for IGR J19308+0530 obtained by phase folding the CAMELOT data on the ephemeris determined in Section 3.1. The light curve displays the typical signature of ellipsoidal variation, with two unequal minima, but in addition asymmetric maxima (O'Connell 1951 and Wilsey & Beaky 2009).

We modelled the i' -band light curve using the XRbinary program written by EL Robinson. A reasonable fit to the data (reduced $\chi^2 \sim 7$, 403 d.o.f.) is obtained with a model assuming an F4V secondary star and including 30 per cent disc contribution to the total light plus a disc hotspot at phase 0.75. The disc veiling in the model is larger than that observed in the spectra, but variability is possible as the photometry was performed one month after the last spectrum was acquired. Similar models with different assumptions about the disc properties (disc radius, height and temperature profile) also give reasonable fits. As we have no indications to single out one

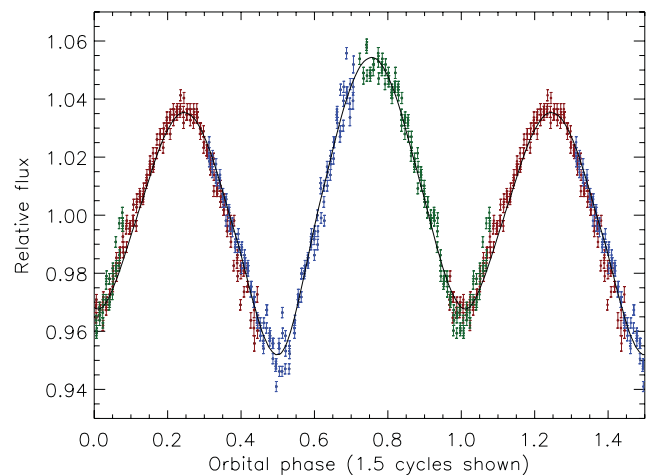


Figure 3. i' -band CAMELOT light curve, folded using the ephemeris from the radial velocity data. The colours indicate the three observing nights (July 30 in red, July 31 in green and August 1 in blue). The drawn line shows a fit with ellipsoidal modulations plus a disc with a bright disc spot.

preferred set of parameters, we do not provide a formal uncertainty on i , but an indicative value of $\sim 52^\circ$ as a guide.

3.3 Upper limits in the radio waveband

We searched for a radio counterpart to IGR J19308+0530 with a Karl G. Jansky Very Large Array observation at 4.6 and 7.9 GHz (120 MHz bandwidth) (proposal ID 10B-238), taken on 2010 August 19 with the array in its most compact D-configuration. The on-source time was 33 min and the data were reduced according to the standard procedures within the Common Astronomy Software Application (McMullin et al. 2007) software package, using the calibrator 3C 286 to set the amplitude scale and J1922+1530 to calibrate the amplitude and phase gains for the target source. IGR J19308+0530 was not detected at either frequency. A 3σ upper limit to the source flux of $54 \mu\text{Jy/beam}$ was derived.

To search for radio pulsations from a potential pulsar in this system, we used the Westerbork Synthesis Radio Telescope and the PuMa2 backend (Karuppusamy, Stappers & van Straten 2008). We observed for 1 h from both 310–380 MHz (Obs. ID 11205182, 2012 August 29) and from 1300–1460 MHz (Obs. ID 11205210, 31 Aug. 2012). The predicted dispersion measure (DM) for a 300 pc distance along this line of sight (see Section 4) is only $\sim 4 \text{ pc cm}^{-3}$ (Cordes & Lazio 2002). For each data set, we used the PRESTO software suite (Ransom 2001) to search a set of trial DMs up to 30 pc cm^{-3} . No obvious radio pulsar signal was detected after an acceleration search. From these observations, we can place conservative flux density limits of $S_{350} < 0.9 \text{ mJy}$ and $S_{1400} < 0.4 \text{ mJy}$ for any pulsar present in the system, assuming it is beamed towards us.

4 DISCUSSION AND CONCLUSION

We performed a dynamical study of the system IGR J19308+0530 through optical spectroscopy and photometry. The optical spectra are dominated by the companion star, with no evidence of irradiation, no emission features visible from the accretion flow besides a partial filling in of the Balmer lines and 10–20 per cent disc contribution to the continuum. The secondary star is most likely of spectral type F4–6 V. Ellipsoidal modulations are detected on the $\sim 14.6 \text{ h}$ orbit. From phase-resolved spectroscopy we measure an extreme value for the binary mass ratio of $q = 1.78 \pm 0.04$. The light-curve modelling provides a reasonable fit to the data with a disc+hotspot model at $i \sim 52^\circ$. Solving the mass function $f(M_2): M_1 \frac{\sin^3 i}{(1+q)^2} = \frac{PK_2^3}{2\pi G} = 0.03 M_\odot$ with this inclination, we obtain the following indicative masses: $M_1 \sim 0.8 M_\odot$ and $M_2 \sim 1.4 M_\odot$. The masses are consistent with a WD accretor and an F4V donor (typical mass of $\sim 1.37 M_\odot$, Mamajek's list 2011²). If the inclination is lower, which we cannot exclude based on these data, the masses will increase, allowing a scenario with a NS primary if $i \lesssim 45^\circ$. However, in this case the companion star would be overmassive for the spectral type, which is unusual for XRB and CVs.

Assuming an F4 V mass donor with a radius equal to that of the Roche lobe for our best estimated masses, the magnitude of the companion is $M_V = 2.7$ in the visual band (half a magnitude brighter than for a typical F4 V star; Mamajek 2011). Comparing with the apparent magnitude of IGR J19308+0530 ($m_V = 10.95 \pm 0.13$, converted from m_{VT} in the Tycho catalogue), we estimate a distance

range of 300–450 pc, for an extinction between $N_H = (0–2.6) \times 10^{21} \text{ cm}^{-2}$ (Dickey & Lockman 1990, where N_H is converted into A_V following Güver & Özel 2009).

Combining the systemic radial velocity with the source proper motion reported in the UCAC3 catalogue (Zacharias et al. 2010), we computed the Galactic space velocity components of IGR J19308+0530 using the method of Johnson & Soderblom (1987). Assuming that the local standard of rest participates in the Galactic rotation at 254 km s^{-1} (Reid et al. 2009) and a distance of $375 \pm 75 \text{ pc}$, the derived peculiar velocity is $45.3 \pm 2.9 \text{ km s}^{-1}$. This rules out a large asymmetric kick from a supernova.

The X-ray luminosity of IGR J19308+0530 measured by *Chandra* in 2007 (Ratti et al. 2010) is $5 \times 10^{29}–4 \times 10^{30} \text{ erg s}^{-1}$, for distance in the above range of 300–450 pc and the corresponding N_H . In the same way, ultraviolet (UV) *Swift* observations provide $4 \times 10^{30}–1 \times 10^{31} \text{ erg s}^{-1} \text{ \AA}^{-1}$ at 2500 \AA . A scenario where IGR J19308+0530 is not in full contact and the X-rays are from coronal activity of the companion seems unlikely. First, coronal activity usually does not produce prolonged high-energy emission, while the source was discovered from a stack of *INTEGRAL* observations. Secondly, coronal activity could explain the observed X-ray luminosity only for the earliest spectral type allowed by the observations combined with very little N_H , as for F stars the ratio between the X-rays and bolometric flux is $\log(L_X/L_{\text{bol}}) \lesssim -4.6$ for $v \sin i \sim 100$ (Walter 1983). Finally, the spectra indicate disc contribution to the continuum, and the emission detected in the Balmer lines shows a slight, variable velocity offset with respect to the rvc of the companion star which is not expected in case they originate from coronal activity. The emission line component also seems weak for a highly active star. A hot WD of $\sim 60\,000 \text{ K}$ alone could account for the UV emission, but not for L_X unless thermonuclear burning is happening on its surface. The few intermediate-mass CVs with long orbital period that are known do appear as super soft sources (SSSs), showing soft X-ray spectra are possibly due to stable hydrogen burning on the WD (e.g., Kahabka 2006). However, with a luminosity of $10^{36}–10^{38} \text{ erg s}^{-1}$, SSSs are much more luminous than what we observe from IGR J19308+0530. As the wind mass-loss expected for the secondary spectral type is low ($\sim 10^{-14} M_\odot \text{ yr}^{-1}$; Cranmer & Saar 2011) wind accretion cannot account for the observed X-ray luminosity.

We conclude that IGR J19308+0530 is most likely in contact, consistent with the ellipsoidal modulations observed in the light curve. This makes the source particularly interesting among the scarcely populated class of IMXBs since it shows Roche lobe overflow at a low accretion rate \dot{m} . This is unusual, as Roche lobe accretion with an intermediate-mass companion and such a large mass ratio is typically considered unstable, with an intense and short-lived accretion phase (e.g., Tauris & van den Heuvel 2006). Donor stars of mass around $1.4 M_\odot$ have thin or non-existent convective envelopes (Verbunt & Zwaan 1981) which implies that the instability does not proceed on a dynamical time-scale. While a convective envelope star would react to mass-loss by expanding, a star with a mostly radiative envelope will shrink, slowing down the mass transfer. However, with a mass ratio of 1.8 the radius of the Roche lobe will reduce faster in response to mass transfer than the radius of the companion, triggering a thermal instability (Tauris & van den Heuvel 2006). Using the binary stellar evolution code originally developed by Eggleton (Yakut & Eggleton 2005, and references therein), we modelled evolutionary tracks that allow for periods of stable Roche lobe accretion on to a WD with masses and orbital periods consistent with our findings, although at higher \dot{m} values than those implied by the L_X (see also the appendix in

² http://www.pas.rochester.edu/~emamajek/EEM_dwarf_UBVIJHK_colours_Teff.dat

Podsiadlowski, Han & Rappaport 2003). The low L_X can be explained if we are observing a short lived phase of low \dot{m} , or if the mass transfer is non-conservative (a fully non-conservative scenario requires a mass-loss rate from the system of 10^{-10} – $10^{-9} M_\odot \text{ yr}^{-1}$). There is currently no direct evidence in favour of or against the presence of mass-loss from the system.

From an observational point of view, an overestimate of q could be due to uncertainties on the limb darkening. However, even assuming a limb darkening of 0 (instead of 0.5) reduces $v \sin i$ by only a few km s^{-1} , still providing a high q of ~ 1.6 .

ACKNOWLEDGEMENTS

PGJ and GN acknowledge support from a VIDI grant from the Netherlands Organization for Scientific Research. We thank T. Marsh for MOLLY, E.L. Robinson for his XRbinary code and F. Verbunt for useful discussion. The National Radio Astronomy Observatory is a facility of the National Science Foundation operated under cooperative agreement by Associated Universities, Inc.

REFERENCES

- Bagnulo S., Jehin E., Ledoux C., Cabanac R., Melo C., Gilmozzi R., ESO Paranal Science Operations Team, 2003, *Messenger*, 114, 10
- Bird A. J. et al., 2006, *ApJ*, 636, 765
- Cordes J. M., Lazio T. J. W., 2002, preprint (arXiv:e-prints)
- Cranmer S. R., Saar S. H., 2011, *ApJ*, 741, 54
- Dickey J. M., Lockman F. J., 1990, *ARA&A*, 28, 215
- Gray D. F., 1992, *Camb. Astrophys. Ser.*, Vol. 20, *The Observation and Analysis of Stellar Photospheres*. Cambridge Univ. Press, Cambridge
- Güver T., Özel F., 2009, *MNRAS*, 400, 2050
- Horne K., Wade R. A., Szkody P., 1986, *MNRAS*, 219, 791
- Johnson D. R. H., Soderblom D. R., 1987, *AJ*, 93, 864
- Kahabka P., 2006, *Adv. Space Res.*, 38, 2836
- Karuppusamy R., Stappers B., van Straten W., 2008, *PASP*, 120, 191
- Knigge C., Baraffe I., Patterson J., 2011, *ApJS*, 194, 28
- Liu Q. Z., van Paradijs J., van den Heuvel E. P. J., 2007, *A&A*, 469, 807
- McCuskey S. W., 1949, *ApJ*, 109, 426
- McMullin J. P., Waters B., Schiebel D., Young W., Golap K., 2007, in Shaw R. A., Hill F., Bell D. J., eds, *ASP Conf. Ser. Vol. 376, Astronomical Data Analysis Software and Systems XVI*. Astron. Soc. Pac., San Francisco, p. 127
- O’Connell D. J. K., 1951, *Publ. Riverview College Obser.*, 2, 85
- Podsiadlowski P., Rappaport S., Pfahl E., 2001, *Astrophysics and Space Science Library (ASSL)*, Vol. 264, *The Influence of Binaries on Stellar Population Studies*. Kluwer, Dordrecht, p. 582
- Podsiadlowski P., Han Z., Rappaport S., 2003, *MNRAS*, 340, 1214
- Ransom S. M., 2001, PhD thesis, Harvard University
- Raskin G. et al., 2011, *A&A*, 526, A69
- Ratti E. M., Bassa C. G., Torres M. A. P., Kuiper L., Miller-Jones J. C. A., Jonker P. G., 2010, *MNRAS*, 408, 1866
- Reid M. J., Menten K. M., Brunthaler A., Zheng X. W., Moscadelli L., Xu Y., 2009, *ApJ*, 693, 397
- Ritter H., Kolb U., 2003, *A&A*, 404, 301
- Rodriguez J., Tomsick J. A., Chaty S., 2008, *A&A*, 482, 731
- Steehgs D., Jonker P. G., 2007, *ApJ*, 669, L85
- Tauris T. M., van den Heuvel E. P. J., 2006, *Formation and Evolution of Compact Stellar X-ray Sources*, Cambridge Univ. Press, Cambridge, p. 623
- Verbunt F., Zwaan C., 1981, *A&A*, 100, L7
- Wade R. A., Horne K., 1988, *ApJ*, 324, 411
- Walter F. M., 1983, *ApJ*, 274, 794
- Wilsey N. J., Beaky M. M., 2009, *Soc. Astron. Sci. Annu. Symp.*, 28, 107
- Wilson R. E., 1953, *General Catalogue of Stellar Radial Velocities*. Carnegie Institute, Washington
- Yakut K., Eggleton P. P., 2005, *ApJ*, 629, 1055
- Zacharias N. et al., 2010, *AJ*, 139, 2184

This paper has been typeset from a \LaTeX file prepared by the author.